
Toward Falsifying Causal Graphs Using a Permutation-Based Test

Elias Eulig^{1,2,*} Atalanti A. Mastakouri³ Patrick Blöbaum³
Michaela Hardt³ Dominik Janzing³

¹German Cancer Research Center (DFKZ) ²Heidelberg University

³Amazon Research Tübingen

elias.eulig@dkfz.de bloebp@amazon.com
{atalanti,milaha,janzind}@amazon.de

Abstract

Understanding the causal relationships among the variables of a system is paramount to explain and control its behaviour. Inferring the causal graph from observational data without interventions, however, requires a lot of strong assumptions that are not always realistic. Even for domain experts it can be challenging to express the causal graph. Therefore, metrics that quantitatively assess the goodness of a causal graph provide helpful checks before using it in downstream tasks. Existing metrics provide an *absolute* number of inconsistencies between the graph and the observed data, and without a baseline, practitioners are left to answer the hard question of how many such inconsistencies are acceptable or expected. Here, we propose a novel consistency metric by constructing a surrogate baseline through node permutations. By comparing the number of inconsistencies with those on the surrogate baseline, we derive an interpretable metric that captures whether the DAG fits significantly better than random. Evaluating on both simulated and real data sets from various domains, including biology and cloud monitoring, we demonstrate that the true DAG is not falsified by our metric, whereas the wrong graphs given by a hypothetical user are likely to be falsified.

1 Introduction

Directed Acyclic Graphs (DAGs) are a core concept of causal reasoning as they form the basis of structural causal models (SCMs) which can be used to predict the effect of interventions in a causal system or even to answer counterfactual questions. For that reason, they have numerous applications, including biology [1, 2, 3], medicine [4] and computer vision [5, 6, 7].

Example 1. Consider the case of cloud monitoring. Here, a graph can capture how latencies and errors propagate in micro-service architectures. Such a graph can be the basis to identify performance bottlenecks, and assist oncall engineers in trouble-shooting operational issues.

Nevertheless, for many real world systems the true causal relationships, represented in the form of a DAG, are often not readily available. If randomized controlled trials are not possible, inferring the DAG from passive observational data alone is a hard problem which rests on strong assumptions on statistical properties (e.g. causal faithfulness), functional relationships, noise distributions, or graph constraints [8, 9, 10, 11, 12, 13]. These assumptions are often violated in practice. Instead of relying on discovery from observational data, domain experts can describe known dependencies in a system. This approach, however, is subject to human error and incomplete knowledge. This is particularly problematic for applications in causal inference, where a wrong graph structure will lead to a wrong estimation of conditional mechanisms in the systems and ultimately to wrong conclusions about the effect of interventions.

* Work done during an internship at Amazon Research Tübingen.

Example 1 (continued). In cloud monitoring, the edge-reversed call graph (obtained from tracing systems) can serve as a first proxy of causal dependencies [14]. That is if service A calls B then latencies and error rates at B can propagate to A . Is this graph correct?

Therefore, efforts towards quantitatively evaluating the consistency of a given graph (either originating from a domain expert or a causal discovery algorithm) using observational data alone are of utmost importance. However, existing attempts towards this direction report the raw number of inconsistencies between DAG and observed data without a baseline of how many such inconsistencies are to be expected in the first place [15, 16]. Striving for zero is unrealistic and the acceptable number of violations depends on many factors including the size and complexity of the graph. On real-world data, the fraction of conditional independence violations for expert-elicited graphs can be surprisingly high due to unidentified confounding or high type I error rates of the conditional independence tests [17] (Fig. 1). In Example 1 such a confounder could be the fluctuating workload of the cluster the microservices run on that affects all latencies in the graph. Other methods require the existence and knowledge of DAGs from a related system [18], or are heavily dependent on a prior over Bayesian graphs [19].

To overcome these drawbacks, in this work we develop a novel metric to evaluate a given graph using observational data alone. Aiming to understand if a number of violations of a user-specified graph is high or low, we compare it against a baseline that we construct by randomly permuting its nodes. Through this comparison we can shed light onto the question if the violations of a user-specified graph are false-positives or point to real deficiencies of the graph.

2 Related Work

In this section, we review existing works that aim to quantify the consistency of a given DAG with observed data.

The R package *dagitty* [15] implements functions to evaluate DAG-dataset consistency by testing conditional independence (CI) relations implied by the graph structure via the d-separation [21] and global Markov condition. However, directly using the number of violations of graph-implied CIs as a metric to evaluate a given graph is not suitable for real-world applications because there exists no nonparametric CI test with valid level¹ over all distributions and thus the probability of type I errors remains unknown in practice [17, Th. 2], c.f. Fig. 1. Therefore, without a baseline comparison, the raw number of violations (absolute or fraction) does not provide the user with a meaningful measure of whether or not the observed inconsistencies of the given graph are significant.

Reynolds et al. [16] validate a given DAG (6 nodes, 8 edges) that relates exposure to spaceflight environment to performance and health outcomes of rats and mice. Together with testing CIs implied by d-separations using *dagitty*, they test whether dependencies implied by the graph lead to marginal dependencies in the observations (faithfulness). Similar to [15] interpreting the results of those tests is challenging, without a baseline comparison. Our metric overcomes this drawback by providing such a baseline comparison to estimate whether the observed inconsistencies are significant.

Pitchforth and Mengersen [18] suggest a number of questions to validate expert elicited Bayesian Networks (BNs). In particular, the authors propose to validate a given BN by verifying that it is similar to BNs from the same domain already established in the literature. Nevertheless, the framework does not provide a quantified measure and many of the questions assume the existence of comparison models in the literature, which may not be available in many domains. In contrast, we propose a quantitative metric, constructed via a surrogate baseline and not reliant on the existence of similar models from the same domain.

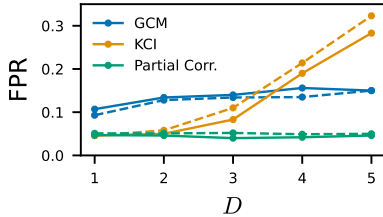


Figure 1: Probability of type I errors at $\alpha = 5\%$ for different sizes D of the conditioning set for one parametric (partial correlation) and two nonparametric CI tests, KCI [20] and GCM [17]. Data (solid: $N = 200$, dashed: $N = 400$) were sampled from gaussian-linear conditionals. More details are given in Supp. B.3.

¹Valid test would mean that for some CI test and sample size N , any distribution from the null is rejected at most with probability of the prespecified significance level α [17].

Finally, numerous works exist on Bayesian structure learning [e.g., 22, 19, 23, 24] where the graph posterior $p(\mathcal{G} \mid \mathcal{D})$ of a graph \mathcal{G} is estimated given some data \mathcal{D} . However, the likelihood $p(\mathcal{D} \mid \mathcal{G})$ remains intractable for general CBNs beyond linear Gaussian and categorical models, and the posterior must be approximated using discrete sampling via Markov chain Monte Carlo (MCMC) methods such as order MCMC [22] or node MCMC. Notable recent work improves on MCMC by approximating the posterior with variational methods [25] or generative flow networks [26]. However, all these methods rely on a prior on the set of DAGs. In contrast, our proposed metric does not rely on a particular prior.

3 Background

This work aims to evaluate the consistency of a given DAG $\hat{\mathcal{G}} = (\mathbf{V}, \hat{\mathcal{E}})$ with vertices $\mathbf{V} = \{1, \dots, n\}$, random variables $\mathbf{X} = \{X_i : i \in \mathbf{V}\}$, and edges $\hat{\mathcal{E}} \subseteq \mathbf{V}^2$ using observations $\mathcal{D} = \{\mathbf{X}^{(1)}, \dots, \mathbf{X}^{(N)}\}$ i.i.d. sampled from the joint distribution $P(\mathbf{X})^2$. We assume the existence of some unknown true causal DAG \mathcal{G}^* and that $P(\mathbf{X})$ satisfies the causal Markov condition relative to \mathcal{G}^* .

In the following, we refer to $X \perp\!\!\!\perp_{\mathcal{D}} Y \mid Z$ as the outcome of a CI test using \mathcal{D} , where X and Y are conditionally independent given Z (and likewise $X \not\perp\!\!\!\perp_{\mathcal{D}} Y \mid Z$ to denote conditional dependency). Note that whether independence is rejected is both a property of \mathcal{D} and the choice of a particular CI test. In this work, to denote that a set of nodes Z d-separates [21] X from Y , we write: $X \perp\!\!\!\perp_{\mathcal{G}} Y \mid Z$.

For some graph $\mathcal{G} = (\mathbf{V}, \mathcal{E})$, we call a node i a parent of node j if $(i, j) \in \mathcal{E}$ and denote with $\text{Pa}_j^{\mathcal{G}}$ the set of all parents of $j \in \mathcal{G}$ ($\text{Pa}_j^{\mathcal{G}} = \emptyset$ iff j is a root node). Furthermore, for nodes i, j if there exists a direct path $i \rightarrow \dots \rightarrow j$ we call i an ancestor of node j and j a descendant of i . We denote with $\text{Anc}_j^{\mathcal{G}}$ the set of all ancestors of $j \in \mathcal{G}$ and with $\text{ND}_i^{\mathcal{G}}$ the set of all non-descendants of $i \in \mathcal{G}$.

The generative process of a system can be modelled using functional causal models (FCMs). We will denote with $\mathfrak{F}(\boldsymbol{\theta}, \mathcal{G})$ an FCM that defines conditional distributions of \mathcal{G} via a set of n structural equations $X_i = f_i(\text{Pa}_i, N_i; \theta_i)$ with $f_i(\cdot; \theta_i), \theta_i \in \boldsymbol{\theta}$ denoting some parameterized function. We further denote with $P^{\mathfrak{F}(\boldsymbol{\theta}, \mathcal{G})}$ the joint distribution induced by such an FCM.

3.1 Tests of Graph Implied (In)dependencies

One common approach to evaluate a DAG using observed data is by means of statistical testing of (in)dependence relations implied by $\hat{\mathcal{G}}$ [e.g. 15, 16]. In the following, we will formally introduce a set of such tests and elaborate on why they are unsuitable to use as a metric directly. In Sec. 4 we will then build upon those existing methods and present a baseline to overcome their drawbacks.

3.1.1 Validating Faithfulness

According to Reichenbach’s common cause principle, if two variables are (unconditionally) dependent, there must exist an unblocked path between them. The opposite implication, however, is only true if P is faithful to \mathcal{G} , i.e. $A \perp\!\!\!\perp_P B \mid C \Rightarrow A \perp\!\!\!\perp_{\mathcal{G}} B \mid C$ for all disjoint vertex sets A, B, C [27].

Definition 3.1 (Marginal dependencies). If P is faithful to \mathcal{G} and there exists an unblocked path between variables X_i, X_j then both must be (unconditionally) dependent, i.e. $X_i \not\perp\!\!\!\perp_P X_j$.

In Reynolds et al. [16] the authors validate a graph by measuring violations of marginal dependencies, i.e. (pairwise) dependencies entailed by the graph which are not represented in the observed data.

Definition 3.2 (Violations of marginal dependencies). We denote with $V_{\text{MD}}^{\hat{\mathcal{G}}, P}$ the set of ordered pairs $(i \in \hat{\mathcal{G}}, X_j \in \text{Anc}_i^{\hat{\mathcal{G}}})$ for which we observe marginal dependency (MD) violations on data \mathcal{D} , i.e.

$$V_{\text{MD}}^{\hat{\mathcal{G}}, \mathcal{D}} = \left\{ i \in \hat{\mathcal{G}}, X_j \in \text{Anc}_i^{\hat{\mathcal{G}}} : X_i \perp\!\!\!\perp_{\mathcal{D}} X_j \right\} . \quad (1)$$

$V_{\text{MD}}^{\hat{\mathcal{G}}, \mathcal{D}}$ detected via Definition 3.2 can have two causes: First, a wrong $\hat{\mathcal{G}}$, where $X_i \not\perp\!\!\!\perp_{\hat{\mathcal{G}}} X_j$ but $X_i \perp\!\!\!\perp_{\mathcal{G}^*} X_j$. Second, a violation of faithfulness, where $X_i \perp\!\!\!\perp_P X_j \not\Rightarrow X_i \perp\!\!\!\perp_{\mathcal{G}^*} X_j$, or close-to-violation of faithfulness $X_i \perp\!\!\!\perp_{\mathcal{D}} X_j \not\Rightarrow X_i \perp\!\!\!\perp_{\mathcal{G}^*} X_j$. While detection of the first cause would be a

²In the following we will assume that this P has a density (w.r.t. a product measure).

viable measure of DAG consistency, it can't be distinguished from the second cause due to P possibly being unfaithful (or close-to-unfaithful) to \mathcal{G}^* . The number of such faithfulness violations is a property of both the graph structure and the parameters of the system and thus highly domain dependent. Already in the population limit, the common ‘probability zero argument’ relies on assuming a probability *density* in the parameter space of conditional distributions [28]. This argument breaks down for priors that assign nonzero probability to more structured mechanisms such as deterministic ones [29]. For finite data, this domain dependence gets even stronger because the probability of accepting independences not entailed by the Markov condition depends on the particular prior on the parameter space, and even for very simple priors over linear relations close-to-violations of faithfulness are not that unlikely [30]. The fact that those close-to-violations of faithfulness are both probable and undetectable when \mathcal{G}^* is unknown renders $V_{\text{MD}}^{\hat{\mathcal{G}}, \mathcal{D}}$ (and with the same argument also possible measures of *conditional* dependencies) unsuitable for measuring DAG consistency directly.

3.1.2 Validating Local Markov Conditions

One of the standard assumptions in causal inference is the causal Markov condition, which allows us to factorize a joint probability distribution $P(\mathbf{X})$ over the variables \mathbf{X} of \mathcal{G} into the product $P(\mathbf{X}) = P(X_1, X_2, \dots, X_n) = \prod_{i=1}^n P(X_i | \text{Pa}_i^{\mathcal{G}})$. We can equivalently formulate this as the parental Markov condition:

Theorem 3.3 (Parental Markov condition [31]). *A probability distribution P is Markov relative to a DAG $\mathcal{G} = (\mathbf{V}, \mathcal{E})$, iff $X_i \perp\!\!\!\perp_P \text{ND}_i^{\mathcal{G}} \setminus \text{Pa}_i^{\mathcal{G}} \mid \text{Pa}_i^{\mathcal{G}}$.*

For the remainder of this work we will use the terms parental Markov condition and local Markov condition (LMC) interchangeably. To test whether a distribution satisfies the parental Markov condition relative to a DAG we can thus list the CIs entailed by the DAG via the graphical d-separation criterion [21] and test whether those are satisfied or violated by the distribution at hand.

Definition 3.4 (Parental triples). For some graph \mathcal{G} , we refer to the ordered triple $(i, j \in \text{ND}_i^{\mathcal{G}}, \text{Pa}_i^{\mathcal{G}})$ as parental triple and denote the set of all such triples implied by \mathcal{G} as $\text{T}_{\text{Pa}}^{\mathcal{G}}$.

According to Theorem 3.3 every parental triple $(i, j, Z) \in \text{T}_{\text{Pa}}^{\mathcal{G}}$ implies the CI $X_i \perp\!\!\!\perp_P X_j \mid Z$. Similar to Textor et al. [15] we will now introduce the notion of violations of LMC:

Definition 3.5 (Violations of LMCs). We denote with $V_{\text{LMC}}^{\hat{\mathcal{G}}, \mathcal{D}}$ the set of triples $(i, j, Z) \in \text{T}_{\text{Pa}}^{\hat{\mathcal{G}}}$, for which (i, j) is an ordered pair, and we observe LMC violations on data \mathcal{D} , i.e.

$$V_{\text{LMC}}^{\hat{\mathcal{G}}, \mathcal{D}} = \left\{ (i, j, Z) \in \text{T}_{\text{Pa}}^{\hat{\mathcal{G}}} : X_i \not\perp\!\!\!\perp_{\mathcal{D}} X_j \mid Z \right\}. \quad (2)$$

Furthermore, we denote the fraction of LMC violations with

$$\phi_{\text{LMC}}^{\hat{\mathcal{G}}, \mathcal{D}} = |V_{\text{LMC}}^{\hat{\mathcal{G}}, \mathcal{D}}| / |\text{T}_{\text{Pa}}^{\hat{\mathcal{G}}}|. \quad (3)$$

Using the two metrics from Definition 3.5 directly to measure the goodness of a user-given graph is not suitable for real-world applications due to the reasons detailed in Sec. 2, particularly the unknown type I error rate of a CI test (c.f. [17] & Fig. 1).

4 Evaluating DAGs via Surrogate Baselines

As discussed, absolute metrics such as $V_{\text{LMC}}^{\hat{\mathcal{G}}, \mathcal{D}}$ or $V_{\text{MD}}^{\hat{\mathcal{G}}, \mathcal{D}}$ are insufficient to measure the consistency of a graph. In the following, we will therefore derive two baselines which can be used as a comparison for the number of (in)dependence violations observed for the given DAG. In Sec. 4.1 we first describe an intuitive approach based on functional causal models. As will be shown, such an approach is not suitable in practice without additional assumptions. In Sec. 4.2 we therefore propose a metric based on the sampling of node-permutations of the given graph and examine some of its properties using group theory. The reader eager to learn about our proposed metric may jump to Sec. 4.2.

4.1 Surrogate Baseline from FCMs

Previously discussed absolute metrics lack a baseline of how many violations to expect for the given graph. E.g. when we observe some number of faithfulness violations, it remains unclear, which

of those are due to a wrong $\hat{\mathcal{G}}$ and which are due to P being (near) unfaithful to \mathcal{G}^* . One could consider constructing a seemingly straightforward baseline as follows: First, sample FCMs $\mathfrak{F}(\hat{\theta}, \hat{\mathcal{G}})$ with random parameters $\hat{\theta}$ and graph structure $\hat{\mathcal{G}}$. Then, compare the number of violations for $\hat{\mathcal{G}}$ and \mathcal{D} to the number of violations observed for $\hat{\mathcal{G}}$ and data i.i.d. sampled from $P^{\mathfrak{F}(\hat{\theta}, \hat{\mathcal{G}})}$ to decide whether the observed faithfulness violations are significant. However, the parameter prior of the sampled FCMs, as well as the chosen model class, plays a crucial role in the violations we observe.

Let us assume that P is induced by some (generally unknown) FCM $\mathfrak{F}(\theta^*, \mathcal{G}^*)$. If we now sample an FCM $\mathfrak{F}(\hat{\theta}, \hat{\mathcal{G}})$ with random parameters $\hat{\theta} \sim \hat{\Theta}$, can we use

$$\mathbb{E}_{\hat{\theta} \sim \hat{\Theta}} \left[V_{\text{LMC}}^{\hat{\mathcal{G}}, P^{\mathfrak{F}(\hat{\theta}, \hat{\mathcal{G}})}} \right], \quad \mathbb{E}_{\hat{\theta} \sim \hat{\Theta}} \left[V_{\text{MD}}^{\hat{\mathcal{G}}, P^{\mathfrak{F}(\hat{\theta}, \hat{\mathcal{G}})}} \right],$$

as a surrogate for the unknown $V_{\text{LMC}}^{\mathcal{G}^*, P}$ or $V_{\text{MD}}^{\mathcal{G}^*, P}$ respectively? Since these values are heavily dependent on the distribution of $\hat{\theta}$ and θ^* , this is not possible in general (see Supp. E for an example).

A random FCM will generally not entail distributions with similar statistical properties as the empirical distribution. This can be enforced by posing additional restrictions on the FCMs. E.g. to derive a surrogate baseline for the number of faithfulness violations we expect for the true DAG, one could fit FCMs \mathfrak{G} to the observed data by choosing powerful models $f_i(\cdot; \theta_i)$, e.g. realized by multi-layer perceptrons (MLPs) and learning the parameters θ_i . If $\hat{\mathcal{G}} = \mathcal{G}^*$, we are guaranteed to observe $V_{\text{MD}}^{\hat{\mathcal{G}}, P^{\mathfrak{G}}} = V_{\text{MD}}^{\hat{\mathcal{G}}, \mathcal{D}}$ for sufficiently powerful function approximators f_i . However, whenever $\hat{\mathcal{G}} \neq \mathcal{G}^*$, we are not guaranteed to do so. To see this, suppose \mathcal{G}^* is given by $X \rightarrow Z, Y$ and $\hat{\mathcal{G}}$ is given by $X \rightarrow Z \leftarrow Y$. The distribution $P^{\mathfrak{G}}$ of a fitted FCM \mathfrak{G} will not satisfy Causal Minimality³ w.r.t. $\hat{\mathcal{G}}$ and we will likely observe the faithfulness violation $Z \perp\!\!\!\perp_{P^{\mathfrak{G}}} Y \not\equiv Z \perp\!\!\!\perp_{\hat{\mathcal{G}}} Y$. Therefore, we conclude that the aforescribed approach of deriving a baseline using either sampled or fitted FCMs is not suitable in practice.

4.2 Surrogate Baseline from Node-Permutations

In the following we will motivate and present a metric based on a permutation test, where we permute the nodes of $\hat{\mathcal{G}}$ and compare the observed violations on $\hat{\mathcal{G}}$ against those observed on permuted graphs. While the remainder of this paper focuses on LMC violations, someone could wonder about its application of faithfulness violations as well. In Supp. G we discuss why the latter is not trivial to construct and analyze different approaches.

4.2.1 Motivation and Hypothesis

The main motivation of our test results from a very skeptical view whether the user specified graph is related to the observed independence structure at all. There are good reasons not to take this for granted. Let us, as an example, consider the dependence structure of services in cloud computing. While it seems intuitively plausible that latencies influence each other along the reverse direction of the dependence graph, it is not clear whether this view is far too simplistic:

Example 1 (continued). Suppose we have a service A that makes two consecutive calls to services B and C . Now, if B 's latency increases, this can not only lead to an increase along the path $B - A$, but also to a timeout that causes A to return an error, as well as skipping the call to C . With the reduced load on C , C 's latency may decrease. Although there is no directed path between B and C , a latency increase at B could thus influence the latency at C . Thus we would find $B \perp\!\!\!\perp_{\hat{\mathcal{G}}} C \not\equiv B \perp\!\!\!\perp_{\mathcal{D}} C$.

In general there can be different reasons why the pattern of observed conditional independences appears unrelated to $\hat{\mathcal{G}}$. On the one hand, the domain ‘expert’ who provided $\hat{\mathcal{G}}$ may have messed up causal links and directions entirely. But even if all the links of $\hat{\mathcal{G}}$ are correct, additional confounding and violations of faithfulness can mess up the independence structure nevertheless. In both cases, DAG and independences appear random *relative to each other* regardless of whether we think the DAG or the pattern of independences (the ‘dual view’) to be random.

³A distribution P over a random vector $X = (X_1, \dots, X_n)$ which is Markovian over a graph \mathcal{G} satisfies Causal Minimality iff $\forall X_j, \forall Y \in \text{Pa}_j^{\mathcal{G}}$ we have that $X_j \not\perp\!\!\!\perp_{P^{\mathcal{G}}} Y \mid \text{Pa}_j^{\mathcal{G}} \setminus \{Y\}$ [32].

We now formalize the concept of being random relative to each other. To this end, let S_n denote the set of permutations π on the vertices $\{1, \dots, n\}$ of some graph \mathcal{G} . For any permutation $\pi \in S_n$ we denote with $\sigma_\pi(\mathcal{G})$ the graph for which the edge $i \rightarrow j$ exists iff $\pi(i) \rightarrow \pi(j)$ exists in \mathcal{G} . Because of the one-to-one correspondence between π and σ we will drop the subscript and in the following refer to $\sigma \in S_{\mathcal{G}}$ as one node-permutation of \mathcal{G} . The most extreme formalization of the skepticism whether the DAG $\hat{\mathcal{G}}$ captures any information about the true causal DAG then reads:

Hypothesis H_0 : The DAG $\hat{\mathcal{G}}$ is drawn uniformly at random from some distribution Q on the set of DAGs that is invariant under permutations of nodes, that is $Q(\mathcal{G}) = Q(\sigma(\mathcal{G}))$ for all $\sigma \in S_{\mathcal{G}}$.

The permutation invariance expresses the hypothesis that the given DAG does not capture anything about the true causal ordering, it is just as good as a DAG in which the ordering of nodes has been randomly permuted. Or, to phrase it in the aforesaid ‘dual’ domain: The pattern of observed independences looks random and to formalize this randomness, we assume a prior on patterns of conditional independences that is invariant with respect to node permutations.

Suppose, we now sample random node-permutations $\sigma \in S_{\hat{\mathcal{G}}}$ of the given graph $\hat{\mathcal{G}}$. In the following, we will examine some of the properties of such a sampling strategy using group theory. Let $O(\hat{\mathcal{G}})$ define the orbit of $\hat{\mathcal{G}}$ under $S_{\hat{\mathcal{G}}}$, i.e., the set of DAGs obtained via permutations. All DAGs in $O(\hat{\mathcal{G}})$ imply the same CIs up to renaming of variables. In particular, the number of the CIs and the size of the conditioning sets remains the same leading to similar statistical properties, e.g. in terms of type I errors (c.f. Fig. 1).

Note that the mapping $S_{\hat{\mathcal{G}}} \rightarrow O(\hat{\mathcal{G}})$ defined by $\sigma \mapsto \sigma(\hat{\mathcal{G}})$ is in general not one-to-one because there will often be a non-trivial subgroup that leaves $\hat{\mathcal{G}}$ invariant (the stabilizer subgroup $\text{Stab}(\hat{\mathcal{G}})$ of $S_{\hat{\mathcal{G}}}$).

Proposition 4.1. *Uniform sampling of permutations from the set of all node permutations $S_{\hat{\mathcal{G}}}$ results in uniform sampling from the DAGs in the orbit $O(\hat{\mathcal{G}})$.*

Proof. From the orbit-stabilizer theorem [33] $|O(\hat{\mathcal{G}})| = |S_{\hat{\mathcal{G}}}|/|\text{Stab}(\hat{\mathcal{G}})|$ and each DAG in $O(\hat{\mathcal{G}})$ has $|\text{Stab}(\hat{\mathcal{G}})|$ many different permutations as pre-images, namely the cosets of $\text{Stab}(\hat{\mathcal{G}})$ in S_n . \square

Further, $O(\hat{\mathcal{G}})$ decomposes into Markov equivalence classes of equal size. This can easily be seen by the same argument when we consider the action of $S_{\hat{\mathcal{G}}}$ on the set of Markov equivalence classes and introduce the corresponding (larger) stabilizer subgroup. This way, our permutation test can also be seen as comparison against *random Markov equivalence classes* in $O(\hat{\mathcal{G}})$.

4.2.2 A Permutation Test to Evaluate DAGs

Motivated by above properties of sampling of node-permutations and our hypothesis H_0 , we consider the number of violations $|V_{\text{LMC}}^{\hat{\mathcal{G}}, \mathcal{D}}|$ as test statistics and build the null via $|V_{\text{LMC}}^{\sigma(\hat{\mathcal{G}}), \mathcal{D}}|$, leading to the metric

$$p_{\text{LMC}}^{\hat{\mathcal{G}}, \mathcal{D}} = \Pr \left(|V_{\text{LMC}}^{\sigma(\hat{\mathcal{G}}), \mathcal{D}}| \leq |V_{\text{LMC}}^{\hat{\mathcal{G}}, \mathcal{D}}| \right). \quad (4)$$

Proposition 4.2. *p_{LMC} is a p-value with type I error control.*

A proof is provided in Supp. F.1. Computing the quantity in (4) using all $n!$ permutations is infeasible for large n . Therefore, we approximate it via Monte Carlo sampling with T random permutations: $\{\sigma_i \sim S_{\hat{\mathcal{G}}}\}_{i=0}^T$. For an estimated p-value we can also report binomial proportion confidence intervals.

Another quantity that proves to be useful in practice is the fraction of DAGs in $O(\hat{\mathcal{G}})$ that are Markov equivalent to $\hat{\mathcal{G}}$. To this end we define

$$V_{\text{TPa}}^{\sigma(\hat{\mathcal{G}}), \hat{\mathcal{G}}} = \{(X_i, X_j, Z) \in \text{TPa}^{\sigma(\hat{\mathcal{G}})} : X_i \not\perp_{\hat{\mathcal{G}}} X_j \mid Z\} \quad (5)$$

as the set of all ordered triples that are parentally d-separated in $\sigma(\hat{\mathcal{G}})$ but not d-separated in $\hat{\mathcal{G}}$.

Proposition 4.3. *Suppose two graphs \mathcal{G}' and \mathcal{G} . If $V_{\text{TPa}}^{\mathcal{G}', \mathcal{G}} = \emptyset$, then \mathcal{G}' and \mathcal{G} are Markov equivalent.*

The proof is provided in Supp. F.2. Using this graphical criterion we can define a second metric

$$p_{\text{TPa}}^{\hat{\mathcal{G}}} := \Pr \left(|V_{\text{TPa}}^{\sigma(\hat{\mathcal{G}}), \mathcal{G}}| \leq |V_{\text{TPa}}^{\hat{\mathcal{G}}}| \right) = \Pr \left(|V_{\text{TPa}}^{\sigma(\hat{\mathcal{G}}), \hat{\mathcal{G}}}| = 0 \right), \quad (6)$$

which can be used to measure how informative the CI structure of $\hat{\mathcal{G}}$ is about the possible causal orderings. If $p_{\text{TPa}}^{\hat{\mathcal{G}}} > \alpha$, for some prespecified threshold α , then the number of Markov equivalent DAGs in $O(\hat{\mathcal{G}})$ is large and consequently $\hat{\mathcal{G}}$ provides us with limited information about the true graph in the sense of testing of CIs. For an information-theoretic interpretation of our test see Supp. D.

Interpretation of p_{LMC} and p_{TPa} The two quantities derived in this section provide orthogonal views on the CIs entailed by a given graph. While p_{LMC} is a measure of how the number of found violations for $\hat{\mathcal{G}}$ compares against a baseline of node-permuted DAGs, p_{TPa} provides us with a measure of its *falsifiability*. If the number of node-permuted DAGs equivalent to $\hat{\mathcal{G}}$ is large, this limits the falsifiability of $\hat{\mathcal{G}}$ via CI testing. Note that by no means the significance of either of the p-values should be interpreted as *acceptance* of $\hat{\mathcal{G}}$. Instead, we propose the following interpretation for practitioners:

1. If $p_{\text{TPa}}^{\hat{\mathcal{G}}} \leq \alpha$, we conclude that the independences entailed by $\hat{\mathcal{G}}$ are ‘characteristic’ in the sense that $\hat{\mathcal{G}}$ is falsifiable by testing implied CIs.
2. If further $p_{\text{LMC}}^{\hat{\mathcal{G}}, \mathcal{D}} \leq \alpha$, we conclude that there is no CI-based evidence against $\hat{\mathcal{G}}$ and that it is significantly better than random DAGs in terms of CI.

5 Experiments

In the following we evaluate our proposed metric on synthetic and real data for which the true DAG is known or a consensus graph is established in the literature. Additionally, we introduce a novel dataset from cloud monitoring where the reversed call graph provides an estimate of the true causal graph (c.f. Example 1), thus providing a useful test beyond synthetic and existing real-world data sets.

5.1 Experimental Setup

We conduct experiments with two different sources of given graphs: Emulated domain experts with partial knowledge of either a subset of nodes or a subset of edges of the true DAG $\mathcal{G}^* = (\mathbf{V}, \mathcal{E}^*)$ and causal discovery algorithms, which are a popular choice to estimate a DAG in the absence of domain expertise. Note that all $\hat{\mathcal{G}}$ in our experiments differ from \mathcal{G}^* in a structured, i.e. non-random, way.

Node Domain Expert (DE- \mathbf{V}) This model mimics the situation where a domain expert knows all causal edges for some subset $K \subseteq \mathbf{V}$ of the nodes in the system and knows the overall sparsity of the DAG. All other edges are assigned randomly between pairs of nodes not both in K . We define different levels of DE- \mathbf{V} to emulate the fraction of nodes for which there exists domain knowledge, i.e. $|K|/|\mathbf{V}|$, where $|K|/|\mathbf{V}| = 0$ corresponds to the situation where the domain expert has no knowledge and $|K|/|\mathbf{V}| = 1$ corresponds to $\hat{\mathcal{G}} = \mathcal{G}^*$. More details are given in Supp. B.1.

Edge Domain Expert (DE- \mathcal{E}) This model mimics a domain expert with edge-specific knowledge about \mathcal{G}^* . To construct $\hat{\mathcal{G}}$, we randomly remove and flip some of the true edges and add some new ones. By construction $\hat{\mathcal{G}}$ of a DE- \mathcal{E} is related to the Structural Hamming Distance (SHD) [34, 35] and thus the desired similarity of a given graph can be controlled by means of the SHD. We characterize different DE- \mathcal{E} by the SHD($\hat{\mathcal{G}}, \mathcal{G}^*$) they entail (or SHD($\hat{\mathcal{G}}, \mathcal{G}^*$)/ $|\mathcal{E}^*|$ to compare systems with different sparsity), where SHD($\hat{\mathcal{G}}, \mathcal{G}^*$)/ $|\mathcal{E}^*| = 0$ corresponds to $\hat{\mathcal{G}} = \mathcal{G}^*$. More details are given in Supp. B.2.

Causal Discovery Algorithms The proposed test can also be applied to DAGs inferred by discovery algorithms. However, as many algorithms use (some of the) CIs either explicitly (constraint-based) or implicitly (score-based) for constructing the DAG, evidence in favor of an inferred DAG can only come from those CIs that were neither used by the algorithm, nor implied (via semi-graphoid axioms [36, 37]) by those CIs used by the algorithm. Nonetheless, we evaluate our test on graphs inferred by LiNGAM [8], CAM [38], and NOTEARS [39]. We chose those algorithms as they are not solely based on CIs (note, however, that e.g. in LiNGAM independence of noise entails CI).

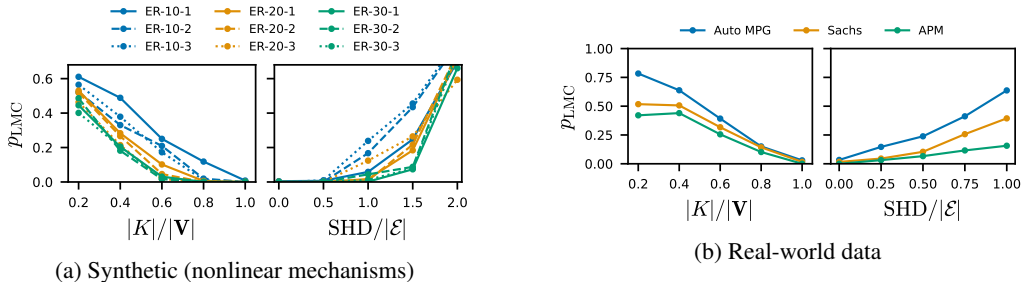


Figure 2: Mean p_{LMC} for (a) random ER graphs and (b) real-world data sets. We simulate given DAGs via DE- \mathbf{V} (left; smaller numbers correspond to less domain knowledge) and DE- \mathcal{E} (right; smaller numbers correspond to more domain knowledge). For all configurations, for the true DAG ($|K|/|\mathbf{V}| = 1$; $SHD/|\mathcal{E}| = 0$), we reject the null that the DAG is as bad as a random node permutation with $\alpha = 1\%$.

5.2 Synthetic Data and Graphs

For evaluating our method on synthetic data we sample random \mathcal{G}^* under the Erdős-Rényi model [40] with $n \in \{10, 20, 30\}$ nodes and an expected degree $d \in \{1, 2, 3\}$, denoted as ER- n - d . To generate synthetic data from \mathcal{G}^* , conditionals are modeled as additive noise models $X_i = f_i(\text{Pa}_i^{\mathcal{G}^*}) + N_i$, $N_i \sim \mathcal{N}(0, 1)$ with f_i either being random (nonlinear) MLPs, or a linear combination of the node’s parents. The exogenous variables are sampled from a normal, uniform, or Gaussian mixture distribution.

For all experiments on synthetic data we sample $T = 10^3$ node permutations and use datasets with $N = 10^3$ observations. To investigate the effect of N and T on p_{LMC} we run ablation studies on nonlinear data with $N, T \in \{10^1, 10^2, 10^3, 10^4\}$. More information on implementation and parameter choices is provided in Supp. B.4.

5.3 Real Data

To evaluate our proposed metric on real world data, we consider three datasets with established consensus graphs serving as ground truth. We provide further details on the data in Supp. B.5.

Protein Signaling Network (Sachs) [1] This open dataset contains quantitative measurements of the expression levels of $n = 11$ phosphorylated proteins and phospholipids in the human primary T cell signaling network. The $N = 7,466$ measurements, corresponding to individual cells, were acquired via intracellular multicolor flow cytometry [1]. The consensus DAG contains 19 edges ($d \approx 3.45$).

Auto MPG [41] The Auto MPG dataset contains eight attributes (three multivalued discrete and five continuous) with the fuel consumption in miles per gallon (mpg) for $N = 398$ unique car models. While the original use of the data was to predict mpg of a car, in line with previous works on causal inference [e.g. 42, 43], we use a consensus network ($n = 6, 9$ edges, $d = 3$).

Application Performance Monitoring (APM) We collect trace data of microservices in a distributed system hosted on Amazon Web Services (AWS). The traces contain latency information on incoming and outbound requests of each service, averaged over 20 min, making observations approximately i.i.d. In total we ran the application for six days, leading to $N = 432$ observations. We test the working hypothesis that the transpose of the dependency graph ($n = 39, 40$ edges, $d \approx 2.05$) of the application is the true causal DAG of the system (for a discussion of this hypothesis, see Sec. 4.2).

6 Results

6.1 Simulated graphs

Nonlinear Mechanisms Figure 2a depicts mean p_{LMC} for 50 synthetic graphs of various size and sparsity with nonlinear mechanisms modeled using random MLPs. As expected, we find that the average p_{LMC} monotonically decreases with increasing amount of domain knowledge for both models of domain experts. When the domain expert has complete knowledge ($\hat{\mathcal{G}} = \mathcal{G}^*$, corresponding to $|K|/|\mathbf{V}| = 1$ for DE- \mathbf{V} and $SHD/|\mathcal{E}| = 0$ for DE- \mathcal{E}), we reject the hypothesis that the DAG is as bad as a random node permutation with significance level $\alpha = 1\%$ for all configurations ($p_{LMC} < 0.005$).

Gaussian-Linear Mechanisms In the supplemental, Fig. A3 we report p_{LMC} for synthetic graphs of various size and sparsity and with linear-gaussian mechanisms. Similar to DAGs with nonlinear mechanisms, we observe that our metric strictly decreases with increasing amount of domain knowledge for both models of domain experts. If $\hat{\mathcal{G}} = \mathcal{G}^*$, we would not reject the true graph using our metric and significance level $\alpha = 1\%$.

Effect of number of sampled permutations and number of observations Further, we investigate the effect of the number of permutations T and sample size N on p_{LMC} for synthetic DAGs with nonlinear mechanisms (Tab. A2). To limit the running time of the experiment, we only evaluate p_{LMC} for the true graph, i.e. $\hat{\mathcal{G}} = \mathcal{G}^*$. Here, we notice that on average our metric is consistently below 0.05, and therefore we would not reject the true graph with significance level $\alpha = 5\%$. The only exception to this are graphs with few nodes (ER-10- d), evaluated on very few ($N = 10$) samples.

6.2 Real World Applications

Figure 2b shows mean p_{LMC} over 50 sampled given DAGs for the three real-world datasets. Similar to the experiments with synthetic data, we find that with increasing amount of domain knowledge (higher $|K|/|V|$, lower $\text{SHD}/|\mathcal{E}|$) p_{LMC} is strictly decreasing. When $\hat{\mathcal{G}} = \mathcal{G}^*$ we reject the hypotheses that the given graphs are as bad as a random node permutation at $\alpha = 5\%$ for all datasets.

Furthermore, we find that for all real-world datasets the fraction of LMC violations $\phi_{\text{LMC}}^{\mathcal{G}^*, \mathcal{D}}$ (3) is between 0.22 and 0.5 (c.f. Tab. 1 & Fig. A6) and thus significantly higher than the expected type I error rate of

5% for the significance level $\alpha = 5\%$ we used for all CI tests. Thus, using $\phi_{\text{LMC}}^{\mathcal{G}^*, \mathcal{D}}$ as a metric, we would falsely reject the true causal graph, naïvely assuming our CI tests would have valid level.

6.3 Causal Discovery Algorithms

While the main scope of this work is to evaluate user-given graphs, we conduct additional experiments with $\hat{\mathcal{G}}$ inferred via causal discovery. On the Sachs et al. [1] data we find that graphs inferred by NOTEARS and LiNGAM are not significantly better than random, whereas graphs inferred by CAM are not falsified using our metric at $\alpha = 1\%$ (Tab. 2). Furthermore, a ranking based on our metric is in accordance with an SHD ranking (NOTEARS > LiNGAM > CAM). Further experimental results on synthetic data are given in Sec. C.3.

7 Discussion

In this work we addressed the lack of a suitable metric to evaluate an estimated DAG on observed data. To this end we discussed two existing absolute metrics that, without a baseline comparison, are difficult to interpret. We therefore proposed two novel metrics, one based on generated samples and one based on node-permutations of the given DAG. We found the former to be unsuitable without strong assumptions and argued in favour of the latter. This metric comprises two tests which measure first, how characteristic a given graph is in the sense that it is falsifiable by testing CIs and second, whether the given graph is significantly better than a random one in terms of CIs.

Some limitations remain which should be addressed in future studies: For very large graphs, our metric is computationally costly as those may entail thousands of CIs. Even though caching computed p-values can significantly speed up computation, it may still be infeasible to evaluate for some very large real-world graphs. Further discussion and analysis of the runtime of our method are discussed in Supp. A. In future studies, we aim to provide specific suggestions for local improvements of the edges that go beyond the simple report of the triplets that result in LMC violations.

Table 1: Mean p_{LMC} and standard deviation for the consensus graphs of the real-world data sets with 95% confidence interval. For $\alpha = 5\%$ we reject the hypotheses that the graphs are as bad as random ones, despite high fractions of violations $\phi_{\text{LMC}}^{\mathcal{G}^*, \mathcal{D}}$ (3).

	Sachs	Auto MPG	APM
$p_{\text{LMC}}^{\mathcal{G}^*, \mathcal{D}}$	0.017 ± 0.011	0.03 ± 0.0052	0.00
95% conf. int.	[0.0086, 0.024]	[0.019, 0.04]	–
$\phi_{\text{LMC}}^{\mathcal{G}^*, \mathcal{D}}$	0.45	0.50	0.22

Table 2: p_{LMC} and SHD for graphs inferred by causal discovery on the Sachs et al. [1] data.

	NOTEARS	LiNGAM	CAM
$p_{\text{LMC}}^{\hat{\mathcal{G}}, \mathcal{D}}$	0.77 ± 0.19	0.35 ± 0.33	0.0091 ± 0.0110
$\text{SHD}/ \mathcal{E} $	2.20 ± 0.23	1.90 ± 0.13	1.50 ± 0.11

References

- [1] K. Sachs, O. Perez, D. Pe'er, D. A. Lauffenburger, and G. P. Nolan, "Causal Protein-Signaling Networks Derived from Multiparameter Single-Cell Data," *Science*, vol. 308, no. 5721, pp. 523–529, Apr. 2005.
- [2] W. Huber, V. J. Carey, L. Long, S. Falcon, and R. Gentleman, "Graphs in molecular biology," *BMC Bioinformatics*, vol. 8, no. Suppl 6, p. S8, Sep. 2007.
- [3] J.-B. Pingault, P. F. O'Reilly, T. Schoeler, G. B. Ploubidis, F. Rijdsdijk, and F. Dudbridge, "Using genetic data to strengthen causal inference in observational research," *Nature Reviews. Genetics*, vol. 19, no. 9, pp. 566–580, Sep. 2018.
- [4] I. Shrier and R. W. Platt, "Reducing bias through directed acyclic graphs," *BMC Medical Research Methodology*, vol. 8, no. 1, p. 70, Oct. 2008.
- [5] L. Wang and H. Sabhi, "Directed Acyclic Graph Kernels for Action Recognition," in *2013 IEEE International Conference on Computer Vision*, Dec. 2013, pp. 3168–3175.
- [6] K. Chalupka, P. Perona, and F. Eberhardt, "Visual causal feature learning," in *Proceedings of the Thirty-First Conference on Uncertainty in Artificial Intelligence*, ser. UAI'15. Arlington, Virginia, USA: AUAI Press, Jul. 2015, pp. 181–190.
- [7] T. Wang, J. Huang, H. Zhang, and Q. Sun, "Visual Commonsense Representation Learning via Causal Inference," in *Proceedings of the IEEE/CVF Conference on Computer Vision and Pattern Recognition Workshops*, 2020, pp. 378–379.
- [8] S. Shimizu, P. O. Hoyer, A. Hyvarinen, and A. Kerminen, "A Linear Non-Gaussian Acyclic Model for Causal Discovery," *Journal of Machine Learning Research*, vol. 7, pp. 2003–2030, 2006.
- [9] J. Peters and P. Bühlmann, "Identifiability of Gaussian structural equation models with equal error variances," *Biometrika*, vol. 101, no. 1, pp. 219–228, 2014.
- [10] D. M. Chickering, "Learning Bayesian Networks is NP-Complete," in *Learning from Data: Artificial Intelligence and Statistics V*, ser. Lecture Notes in Statistics, D. Fisher and H.-J. Lenz, Eds. New York, NY: Springer, 1996, pp. 121–130.
- [11] D. M. Chickering, D. Heckerman, and C. Meek, "Large-Sample Learning of Bayesian Networks is NP-Hard," *Journal of Machine Learning Research*, vol. 5, pp. 1287–1330, 2004.
- [12] T. Claassen, J. M. Mooij, and T. Heskes, "Learning Sparse Causal Models is not NP-hard," in *Conference on Uncertainty in Artificial Intelligence*, 2013, p. 10.
- [13] J. M. Mooij, J. Peters, D. Janzing, J. Zscheischler, and B. Schölkopf, "Distinguishing Cause from Effect Using Observational Data: Methods and Benchmarks," *Journal of Machine Learning Research*, vol. 17, no. 32, pp. 1–102, 2016.
- [14] K. Budhathoki, L. Minorics, P. Bloebaum, and D. Janzing, "Causal structure-based root cause analysis of outliers," in *Proceedings of the 39th International Conference on Machine Learning*. PMLR, Jun. 2022, pp. 2357–2369.
- [15] J. Textor, B. van der Zander, M. S. Gilthorpe, M. Liskiewicz, and G. T. Ellison, "Robust causal inference using directed acyclic graphs: The R package 'dagitty'," *International Journal of Epidemiology*, vol. 45, no. 6, pp. 1887–1894, Dec. 2016.
- [16] R. J. Reynolds, R. T. Scott, R. T. Turner, U. T. Iwaniec, M. L. Bouxsein, L. M. Sanders, and E. L. Antonsen, "Validating Causal Diagrams of Human Health Risks for Spaceflight: An Example Using Bone Data from Rodents," *Biomedicines*, vol. 10, no. 9, p. 2187, Sep. 2022.
- [17] R. D. Shah and J. Peters, "The Hardness of Conditional Independence Testing and the Generalised Covariance Measure," *The Annals of Statistics*, vol. 48, no. 3, Jun. 2020.
- [18] J. Pitchforth and K. Mengersen, "A proposed validation framework for expert elicited Bayesian Networks," *Expert Systems with Applications*, vol. 40, no. 1, pp. 162–167, Jan. 2013.
- [19] D. M. Chickering, "Optimal Structure Identification With Greedy Search," *Journal of Machine Learning Research*, vol. 3, pp. 507–554, 2002.
- [20] K. Zhang, J. Peters, D. Janzing, and B. Schölkopf, "Kernel-based conditional independence test and application in causal discovery," in *Proceedings of the Twenty-Seventh Conference on Uncertainty in Artificial Intelligence*, ser. UAI'11. Arlington, Virginia, USA: AUAI Press, Jul. 2011, pp. 804–813.

- [21] J. Pearl, *Probabilistic Reasoning in Intelligent Systems: Networks of Plausible Inference*, ser. The Morgan Kaufmann Series in Representation and Reasoning. San Francisco, California: Morgan Kaufmann, 1988.
- [22] D. Madigan, J. York, and D. Allard, “Bayesian Graphical Models for Discrete Data,” *International Statistical Review / Revue Internationale de Statistique*, vol. 63, no. 2, pp. 215–232, 1995.
- [23] N. Friedman, “Being Bayesian About Network Structure. A Bayesian Approach to Structure Discovery in Bayesian Networks,” *Machine Learning*, p. 31, 2003.
- [24] J. Kuipers and G. Moffa, “Uniform random generation of large acyclic digraphs,” Tech. Rep., Nov. 2013.
- [25] L. Lorch, J. Rothfuss, B. Schölkopf, and A. Krause, “DiBS: Differentiable Bayesian Structure Learning,” Dec. 2021.
- [26] T. Deleu, A. Góis, C. Emezue, M. Rankawat, S. Lacoste-Julien, S. Bauer, and Y. Bengio, “Bayesian Structure Learning with Generative Flow Networks,” Jun. 2022.
- [27] P. Spirtes, C. Glymour, and R. Scheines, *Causation, Prediction, and Search*, 2nd ed., ser. Adaptive Computation and Machine Learning. Cambridge, MA: MIT Press, 2000.
- [28] C. Meek, “Strong completeness and faithfulness in Bayesian networks,” in *Proceedings of the Eleventh Conference on Uncertainty in Artificial Intelligence*, ser. UAI’95. San Francisco, CA, USA: Morgan Kaufmann Publishers Inc., Aug. 1995, pp. 411–418.
- [29] J. Lemeire, S. Meganck, F. Cartella, and T. Liu, “Conservative independence-based causal structure learning in absence of adjacency faithfulness,” *International Journal of Approximate Reasoning*, vol. 53, no. 9, pp. 1305–1325, Dec. 2012.
- [30] C. Uhler, G. Raskutti, P. Bühlmann, and B. Yu, “Geometry of the faithfulness assumption in causal inference,” *The Annals of Statistics*, vol. 41, no. 2, Apr. 2013.
- [31] J. Pearl, *Causality*, 2nd ed. Cambridge: Cambridge University Press, 2009.
- [32] J. Peters, D. Janzing, and B. Schölkopf, *Elements of Causal Inference: Foundations and Learning Algorithms*, ser. Adaptive Computation and Machine Learning Series, F. Bach, Ed. Cambridge, MA, USA: MIT Press, Nov. 2017.
- [33] H. E. Rose, “Action and the Orbit–Stabiliser Theorem,” in *A Course on Finite Groups*, ser. Universitext, H. Rose, Ed. London: Springer, 2009, pp. 91–111.
- [34] S. Acid and L. M. de Campos, “Searching for Bayesian Network Structures in the Space of Restricted Acyclic Partially Directed Graphs,” *Journal of Artificial Intelligence Research*, vol. 18, pp. 445–490, May 2003.
- [35] I. Tsamardinos, L. E. Brown, and C. F. Aliferis, “The max-min hill-climbing Bayesian network structure learning algorithm,” *Machine Learning*, vol. 65, no. 1, pp. 31–78, Oct. 2006.
- [36] J. Pearl and A. Paz, “Graphoids: Graph-based logic for reasoning about relevance relations or when would x tell you more about y if you already know z?” in *Proceedings of the 7th European Conference on Artificial Intelligence - Volume 2*, ser. ECAI’86. United Kingdom: North-Holland, Jul. 1986, pp. 357–363.
- [37] D. Geiger, T. Verma, and J. Pearl, “Identifying independence in bayesian networks,” *Networks*, vol. 20, no. 5, pp. 507–534, 1990.
- [38] P. Bühlmann, J. Peters, and J. Ernest, “CAM: Causal additive models, high-dimensional order search and penalized regression,” *The Annals of Statistics*, vol. 42, no. 6, Dec. 2014.
- [39] X. Zheng, B. Aragam, P. K. Ravikumar, and E. P. Xing, “DAGs with NO TEARS: Continuous Optimization for Structure Learning,” in *Advances in Neural Information Processing Systems*, vol. 31. Curran Associates, Inc., 2018.
- [40] P. Erdős and A. Rényi, “On Random Graphs I,” *Publicationes Mathematicae Debrecen*, vol. 6, pp. 290–297, 1959.
- [41] J. R. Quinlan, “Combining instance-based and model-based learning,” in *Proceedings of the Tenth International Conference on International Conference on Machine Learning*, ser. ICML’93. San Francisco, CA, USA: Morgan Kaufmann Publishers Inc., Jul. 1993, pp. 236–243.
- [42] J. Wang and K. Mueller, “Visual Causality Analysis Made Practical,” in *2017 IEEE Conference on Visual Analytics Science and Technology (VAST)*. Phoenix, AZ: IEEE, Oct. 2017, pp. 151–161.

- [43] T. Teshima and M. Sugiyama, “Incorporating Causal Graphical Prior Knowledge into Predictive Modeling via Simple Data Augmentation,” in *37th Conference on Uncertainty in Artificial Intelligence*, 2021, p. 11.
- [44] J. Ramsey and B. Andrews, “FASK with Interventional Knowledge Recovers Edges from the Sachs Model,” May 2018.
- [45] C. Glymour, K. Zhang, and P. Spirtes, “Review of Causal Discovery Methods Based on Graphical Models,” *Frontiers in Genetics*, vol. 10, 2019.
- [46] S. L. Lauritzen, A. P. Dawid, B. N. Larsen, and H.-G. Leimer, “Independence properties of directed markov fields,” *Networks*, vol. 20, no. 5, pp. 491–505, 1990.
- [47] S. Lauritzen, *Lecture Notes: Lectures on Graphical Models*. University of Copenhagen, 2020, vol. 3.
- [48] L. Henckel, E. Perković, and M. H. Maathuis, “Graphical Criteria for Efficient Total Effect Estimation via Adjustment in Causal Linear Models,” *Journal of the Royal Statistical Society: Series B (Statistical Methodology)*, vol. 84, no. 2, pp. 579–599, Apr. 2022.

Supplementary Material: Toward Falsifying Causal Graphs Using a Permutation-Based Test

A Algorithms

Recall that T is the number of permutations we sample. For each permutation we iterate through the nodes and check conditional independence of the node and each non-descendent conditioned on the parents. For n nodes in the graph we thus require $\mathcal{O}(T \cdot n^2)$ independence test. The complexity of each such test further depends on the degree of the nodes that represent the conditioning set. A practical improvement in case the number of violations is small is to start out with testing for each node i whether $X_i \perp\!\!\!\perp_{\mathcal{D}} \text{ND}_i^{\mathcal{G}} \setminus \text{Pa}_i^{\mathcal{G}} \mid \text{Pa}_i^{\mathcal{G}}$. If yes we can move on to the next node. If not, then we have to do some more work to find out exactly how many nondescendents are dependent. This can be done by recursively splitting the set of nondescendents for which a violation was found and recursing on those with violations. That number of group conditional independence test is $\mathcal{O}(|V_{\text{LMC}}^{\mathcal{G},P}| \cdot \log(n^2))$. It is worth pointing out though that the complexity of the test depends on the group size. So the time savings do not just depend on the number of violations but also the exact test that is used. Reducing the number of tests not only reduces the running time but also the overall type-I error. Alternatively, we can consider sampling from $T_{\text{Pa}}^{\hat{\mathcal{G}}}$ to estimate the number of violations rather than computing it exactly.

In Tab. A1 we report runtimes of our method (with $T = 1000$) for the three real-world datasets considered in our study. We find that on all data sets our test runs in under 16 minutes which is reasonable compared to the time it takes to come up with a graph in the first place. Note that $T > 1/\alpha$ permutations for significance level α are only necessary if we seek a precise estimate of p_{LMC} (see Tab. 1 for confidence intervals). Rejecting H_0 at α only requires $1/\alpha$ permutations (c.f. Sec. F.1).

B Experiments

B.1 Node Domain Expert

Here, we outline the procedure by which the given DAG by a node domain expert Fig. A1b is constructed from the true DAG \mathcal{G}^* :

- (1) Extracting a random subset $K \subseteq \mathbf{V}$ of the nodes (these are the nodes of which the domain expert has complete knowledge), for which

$$\forall i, \forall j \in K : (i, j) \in \mathcal{E}^* \Leftrightarrow (i, j) \in \hat{\mathcal{E}}, \text{ and}$$

- (2) all other edges $(i, j) \in \mathcal{E}^*$, $i \notin K \vee j \notin K$ are randomly shuffled while ensuring that $\hat{\mathcal{G}}$ remains acyclic.

B.2 Edge Domain Expert

Starting from the true DAG \mathcal{G}^* , to construct $\hat{\mathcal{G}}$, some edges N , $N \cap \mathcal{E}^* = \emptyset$ are added, $M \subseteq \mathcal{E}^*$ are removed, and $L \subseteq \mathcal{E}^* \setminus M$ are flipped. Similar to DE-V we further ensure that $\hat{\mathcal{G}}$ has the same sparsity as \mathcal{G}^* by enforcing $|N| = |M|$. Using $\mathcal{E}^f = \{(j, i) : (i, j) \in \mathcal{E}^*\}$ to denote the set of flipped edges, the given DAG $\hat{\mathcal{G}} = (\mathbf{V}, \hat{\mathcal{E}})$ is constructed by:

Table A1: Runtime (mean \pm std over ten runs) of our test on a single machine with 24 cores.

	Sachs	Auto MPG	APM
Runtime [s]	216.0 \pm 1.1	15.2 \pm 0.2	964.5 \pm 25.5

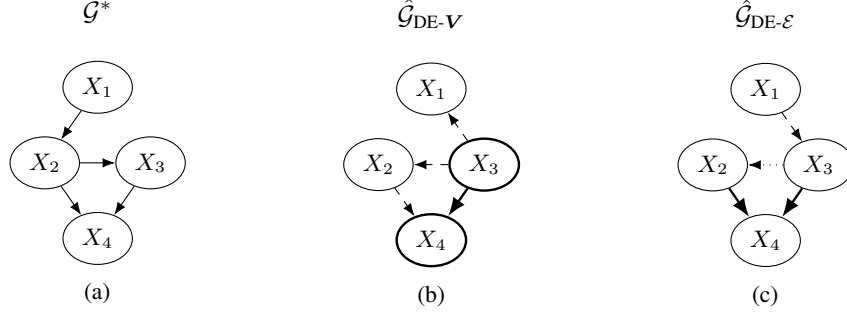


Figure A1: (a) True DAG \mathcal{G}^* ; (b) $\hat{\mathcal{G}}$ from a DE- \mathbf{V} , where $K = \{X_3, X_4\}$ (\rightarrow) and the remaining 3 edges are randomly shuffled ($- \rightarrow$); (c) $\hat{\mathcal{G}}$ from a DE- \mathcal{E} , where $N = \{(X_1, X_3)\}$ ($- \rightarrow$), $M = \{(X_1, X_2)\}$, and $L = \{(X_2, X_3)\}$ ($\cdots \rightarrow$).

- (1) Adding a random set of edges $N \subset \mathbf{V}^2 \setminus (\mathcal{E}^* \cup \mathcal{E}^f)$

$$\forall (i, j) \in N : (i, j) \notin \mathcal{E}^* \Leftrightarrow (i, j) \in \hat{\mathcal{E}}, \text{ and}$$

- (2) removing a random subset $M \subset \mathcal{E}^*$ of the edges:

$$\forall (i, j) \in M : (i, j) \in \mathcal{E}^* \Leftrightarrow (i, j) \notin \hat{\mathcal{E}}, \text{ and}$$

- (3) flipping a random subset $L \subset \mathcal{E}^* \setminus M$ of the edges:

$$\forall (i, j) \in L : (i, j) \in \mathcal{E}^* \Leftrightarrow (j, i) \in \hat{\mathcal{E}}.$$

By construction $\hat{\mathcal{G}}$ of a DE- \mathcal{E} is related to the Structural Hamming Distance (SHD)⁴ [34, 35], via $\text{SHD}(\hat{\mathcal{G}}, \mathcal{G}^*) = |N| + |M| + |L|$, and thus the desired similarity of a given graph can be controlled by means of the SHD. We characterize different DE- \mathcal{E} by the $\text{SHD}(\hat{\mathcal{G}}, \mathcal{G}^*)$ they entail (or $\text{SHD}(\hat{\mathcal{G}}, \mathcal{G}^*)/|\mathcal{E}^*|$ to compare systems with different sparsity), where $\text{SHD}(\hat{\mathcal{G}}, \mathcal{G}^*)/|\mathcal{E}^*| = 0$ corresponds to $\hat{\mathcal{G}} = \mathcal{G}^*$.

B.3 False Positive Rate of Different CI Tests

In Fig. 1 we show the probability of Type I errors for different sizes D of the conditioning set $\{Z_1, Z_2, \dots, Z_D\}$ for one parametric (partial correlation) and two nonparametric CI tests, the *Kernel-based Conditional Independence Test (KCI)* [20] and a test based on the *Generalized Covariance Measure (GCM)* [17]. In our experiment, Z_i were i.i.d. standard Gaussian and X and Y were generated from Z_1 alone via $\beta Z + N$ with $\beta \in \text{U}(-1, 1)$, $N \sim \mathcal{N}(0, 1)$ independent across X, Y . We used GCM with boosted regression trees as the regression method (as in all other experiments in this work) and neither learned the hyperparameters for GCM nor for KCI for comparability. The reported FPR is over 1000 random replications.

B.4 Synthetic Data

For all experiments on synthetic data we sample $T = 10^3$ node permutations and use datasets with $N = 10^3$ observations. For experiments on graphs inferred via causal discovery algorithms we infer the graph on $N = 10^3$ independent samples. To investigate the effect of N and T on p_{LMC} we run ablation studies with $N, T \in \{10^1, 10^2, 10^3, 10^4\}$.

Generation of Random DAGs To sample random DAGs we first generate random graphs under the Erdős-Rényi model [40] and convert a graph to a DAG by only keeping the lower triangle of its adjacency matrix.

⁴We here consider the version of SHD in which anticausal edges are counted once.

Linear Mechanisms For simulating linear relationships between nodes, we model conditionals as ANMs

$$X_i = f_i(\text{Pa}_i^{\mathcal{G}^t}) + N_i, f_i = \sum_{j=0}^M w_j \left(\text{Pa}_i^{\mathcal{G}^t} \right)_j, \quad (7)$$

where $M = |\text{Pa}_{X_i}^{\mathcal{G}^t}|$, and $w_j \sim \text{U}(-1.0, 1.0)$. For all synthetic data sets with linear mechanisms we utilize a CI test of partial correlation to evaluate our metric.

Nonlinear Mechanisms For simulating nonlinear relationships between nodes we use 3-layer MLPs with randomly initialized weights:

$$f_i(\text{Pa}_i^{\mathcal{G}^*}) = \sigma \left(\sum_{l=0}^O w_{il}^{(3)} \sigma \left(\sum_{k=0}^N w_{lk}^{(2)} \sigma \left(\sum_{j=0}^M w_{kj}^{(1)} \left(\text{Pa}_i^{\mathcal{G}^*} \right)_j \right) \right) \right), \quad (8)$$

where σ denotes the sigmoid function, $N, O \stackrel{\text{i.i.d.}}{\sim} \text{U}(2, 100)$, and entries in the weight matrices $w_{ij}^{(k)} \sim \text{U}(-5.0, 5.0)$. For all synthetic data sets with nonlinear mechanisms we utilize a CI test based on the generalised covariance measure [17] with boosted decision trees as the regression model.

B.5 Real Data

The confidence intervals in Tab. 1 are computed via

$$\text{confidence interval} = \hat{p}_{\text{LMC}} \pm z \sqrt{\frac{\hat{p}_{\text{LMC}}(1 - \hat{p}_{\text{LMC}})}{T}}, \quad (9)$$

where \hat{p}_{LMC} denotes a p-value estimated using T permutations and z denotes the z -score. In all experiments on real-world data we set $T = 1000$.

For the **Protein Signaling Network** dataset, we define the true DAG (Fig. A2c) according to the ‘‘extended expert model’’ described in [1, 44, 45]. A pairwise scatter plot and histograms of the 11 variables is provided in Fig. A2d. Because of the relatively large number of samples, we validate LMCs using a CI test based on the generalised covariance measure [17] with boosted decision trees as the regression model.

For the **Auto MPG** dataset, we define the true DAG (Fig. A2a) based on known causal relationships and similar to the ones described in Wang and Mueller [42], Teshima and Sugiyama [43]. In Fig. A2b we provide a pairwise scatter plot and histograms of the 6 variables we used to model the system. Due to the discrete features we employ a kernel-based CI test [20] to validate LMCs.

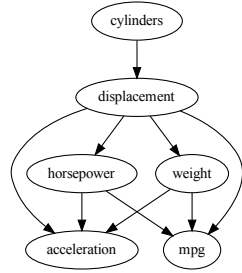
For the **Application Performance Monitoring** dataset, we employ the PetAdoptions application as introduced by AWS in an online workshop⁵ and available on GitHub⁶. We ran the application for six days and collected latency data of each microservice averaged over 20 min, leading to a total of $N = 432$ datapoints which we treat as i.i.d. for our following experiments (see Fig. A2f for a pairwise scatter plot and histogram of the variables). In our experiments, we assume the transpose of the dependency graph of the application to be the causal DAG of the system Fig. A2e. Note, that for some of the nodes no data was recorded, or the data had missing values (due to less frequent calls to the respective microservice). In our experiments we excluded those nodes from the graph evaluation. Because of the large number of graph-implied independencies we employ a CI test based on the generalized covariance measure using boosted decision trees as regression model.

C Additional Experimental Results

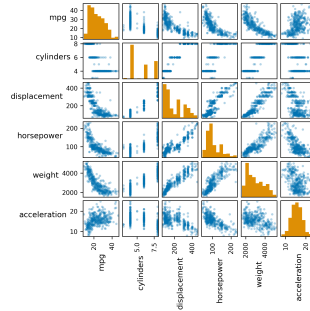
In the following we present further experimental results for both synthetic (Supp. C.1) and real data (Supp. C.1), as well as on graphs inferred via causal discovery algorithms (Supp. C.3).

⁵<https://catalog.workshops.aws/observability/>

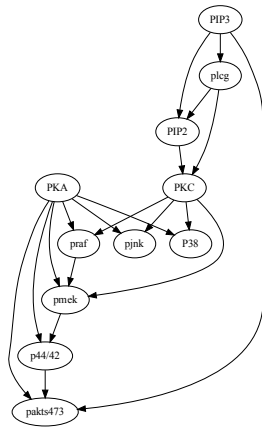
⁶<https://github.com/aws-samples/one-observability-demo/tree/main/PetAdoptions/petsite/petsite/Controllers>



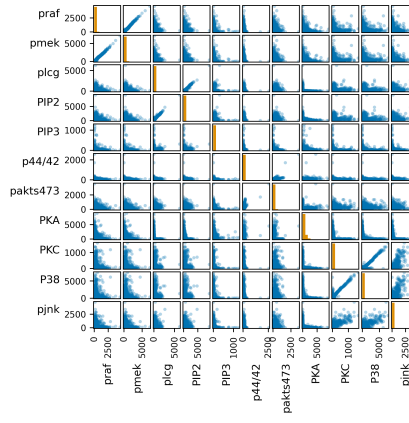
(a)



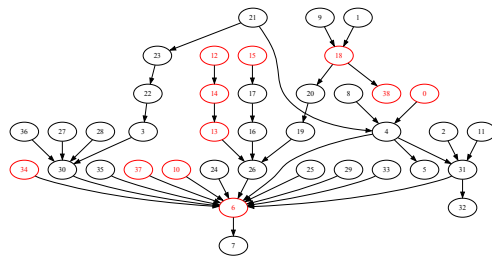
(b)



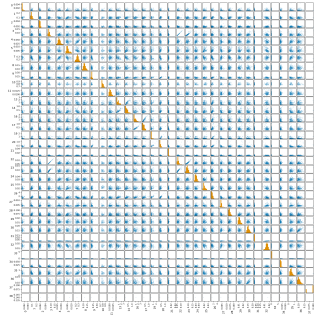
(c)



(d)



(e)



(f)

Figure A2: (a) \mathcal{G}^t for the Auto MPG data; (b) Pairwise scatter plot and histograms of the variables in the Auto MPG data from Quinlan [41]; (c) \mathcal{G}^t for the protein signaling networks data; (d) Pairwise scatter plot and histograms of the 11 variables in the protein signaling network data from Sachs et al. [1]; (e) \mathcal{G}^t for the APM data with excluded nodes marked in red; (f) Pairwise scatter plot and histograms of the variables in the APM data from.

Table A2: Effect of number of observations N and number of sampled permutations T on our metric. We evaluate p_{LMC} of randomly sampled ER graphs with varying number of nodes n and sparsity d for which data is generated via nonlinear SCMs (c.f. Sec. 5.2). The reported numbers are averages over 50 random samples.

n	d	Number of permutations (T)				Number of observations (N)			
		10	100	1000	10000	10	100	1000	10000
10	1	6×10^{-3}	9.4×10^{-3}	9.36×10^{-3}	8.90×10^{-3}	1.04×10^{-1}	8.4×10^{-3}	2.8×10^{-3}	2×10^{-3}
	2	0	0	0	2.2×10^{-5}	8.49×10^{-2}	3.6×10^{-4}	2×10^{-5}	0
	3	0	0	0	0	1.00×10^{-1}	4×10^{-4}	2×10^{-5}	0
20	1	0	0	4×10^{-5}	4.4×10^{-5}	7.2×10^{-3}	2×10^{-5}	0	0
	2	0	0	0	0	2.5×10^{-3}	0	0	0
	3	0	0	0	0	9.8×10^{-3}	0	0	0
30	1	0	0	0	0	3.3×10^{-3}	5.2×10^{-4}	0	0
	2	0	0	0	0	7.8×10^{-4}	0	0	0
	3	0	0	0	0	3.4×10^{-3}	0	0	0

C.1 Synthetic Data

Gaussian-Linear Mechanisms Figure A3 shows p_{LMC} (c.f. Sec. 4.2) for synthetic graphs of various size and sparsity and with linear-gaussian mechanisms, where CIs were tested via partial correlation. As expected, we find that the average p_{LMC} monotonically decreases with increasing amount of domain knowledge for both models of domain experts. When the domain expert has complete knowledge of the underlying system ($\hat{\mathcal{G}} = \mathcal{G}^*$, corresponding to $|K|/|V| = 1$ for DE- V and $\text{SHD}/|\mathcal{E}| = 0$ for DE- \mathcal{E}), we reject the hypothesis that the DAG is as bad as a random node permutation with significance level $\alpha = 1\%$ for all configurations.

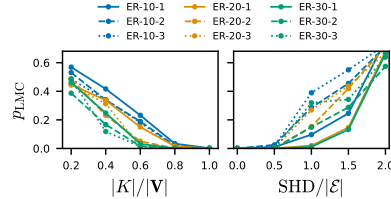


Figure A3: p_{LMC} for random ER graphs with Gaussian-linear mechanisms.

Effect of number of sampled permutations and number of observations In Tab. A2 we report results on the effect of the number of observations and the number of sampled permutations on our proposed metric for ER graphs with nonlinear mechanisms and of different size and sparsity. In Fig. A4 and A5, we show the accumulated histograms of fractions of violations for both domain experts on random ER graphs with varying density and size for linear and nonlinear mechanisms, respectively.

C.2 Real Data

In Fig. A6 we provide histograms of the number of fractions of LMC violations for the three real-world datasets.

C.3 Causal Discovery Algorithms

This work is mainly concerned with evaluating user-given graphs, i.e. graphs originating from a domain expert that has knowledge about some of the variables/edges of the underlying causal system. However, if such domain knowledge is unavailable, practitioners may infer the graph from observational data using causal discovery. To test the applicability of our metric to such graphs (for arguments on why this applicability may be limited, c.f. Sec. 5.1), we conduct additional experiments using graphs inferred via LiNGAM [8], CAM [38], and NOTEARS [39] on synthetic \mathcal{G}^* from ER- n - d , $n \in \{10, 20, 30\}$, $d \in \{1, 2, 3\}$ with nonlinear mechanisms ($N = 2000$ samples) and the protein signaling network dataset [1].⁷ We randomly choose 50% of the samples to infer the graph

⁷For LiNGAM and CAM, we use implementations from the Causal Discovery Toolbox (<https://github.com/FenTechSolutions/CausalDiscoveryToolbox>). For NOTEARS we use the authors implementation available at <https://github.com/xunzheng/NOTEARS>.

and the remaining samples to evaluate using our metric (Fig. A7). We repeated experiments (inferring using causal discovery + evaluation with our metric) ten times for each configuration.

On synthetic data (Fig. A7a) we find that our metric is positively correlated with $\text{SHD}/|\mathcal{E}|$ for CAM ($r = 0.62, p < 0.001$), but not for NOTEARS and LiNGAM. On both, synthetic and real data we find that a ranking of the causal discovery algorithms based on our metric agrees with a ranking based on $\text{SHD}/|\mathcal{E}|$ (Tab. 2 and A3).

Table A3: p_{LMC} and SHD for graphs inferred by causal discovery on synthetic data with nonlinear mechanisms.

	NOTEARS	LiNGAM	CAM
$p_{\text{LMC}}^{\hat{\mathcal{G}}, \mathcal{D}}$	0.014 ± 0.044	0.0048 ± 0.0240	0.031 ± 0.110
$\text{SHD}/ \mathcal{E} $	1.70 ± 0.71	1.50 ± 0.54	3.8 ± 4.3

D An Information-theoretic View on the Node Permutation Test

Let us consider the following scenario. Let the variables of $\hat{\mathcal{G}}$ be labeled according to some topological ordering of $\hat{\mathcal{G}}$. This ordering may not be valid as topological ordering of \mathcal{G}^* . Let π some random choice among those re-orderings of nodes that result in a topological ordering of \mathcal{G}^* .

We now state an assumption that we will later interpret with a grain of salt:

Assumption 1. $\sigma_{\pi}(\hat{\mathcal{G}})$ does not show more violations of LMC than $(\hat{\mathcal{G}})$.

The idea is that $\hat{\mathcal{G}}$ is not that far from \mathcal{G}^* that getting nodes into a valid causal ordering results in even more violations than the wrong causal ordering. Since we only estimate the number of violations for large n anyway, we can read Assumption 1 also in the sense of ‘does not show *significantly* more violations’.

Together with Assumption 1, $\hat{\mathcal{G}}$ and the independence structure reduces the set of possible orderings π by the factor $p_{\text{LMC}}^{\hat{\mathcal{G}}, \mathcal{D}}$. Starting with a uniform prior over S_n , $\hat{\mathcal{G}}$ and the observed independences thus contain the Shannon information $-\log p_{\text{LMC}}^{\hat{\mathcal{G}}, \mathcal{D}}$ about π . Likewise, $-\log p_{\text{TPa}}^{\hat{\mathcal{G}}}$ is the amount of information $\hat{\mathcal{G}}$ and the independence structure provide about the valid causal ordering.

E Sampling FCMs to Build a Surrogate Baseline

Let us assume that P is induced by some (generally unknown) FCM $\mathfrak{F}(\theta^*, \mathcal{G}^*)$. If we now sample an FCM $\mathfrak{F}(\hat{\theta}, \hat{\mathcal{G}})$ with random parameters $\hat{\theta} \sim \hat{\Theta}$, can we use

$$\mathbb{E}_{\hat{\theta} \sim \hat{\Theta}} \left[V_{\text{LMC}}^{\hat{\mathcal{G}}, P^{\mathfrak{F}}(\hat{\theta}, \hat{\mathcal{G}})} \right], \quad \mathbb{E}_{\hat{\theta} \sim \hat{\Theta}} \left[V_{\text{MD}}^{\hat{\mathcal{G}}, P^{\mathfrak{F}}(\hat{\theta}, \hat{\mathcal{G}})} \right],$$

as a surrogate for the unknown $V_{\text{LMC}}^{\mathcal{G}^*, P}$ or $V_{\text{MD}}^{\mathcal{G}^*, P}$ respectively? The following example shows that for $V_{\text{MD}}^{\hat{\mathcal{G}}, P^{\mathfrak{F}}(\hat{\theta}, \hat{\mathcal{G}})}$ this is not possible in general if the distributions of $\hat{\theta}$ and θ^* have different priors.

Example 2. Assume some true DAG \mathcal{G}^* with FCM $\mathfrak{T} = \mathfrak{F}(\theta^*, \mathcal{G}^*)$ being a linear-additive noise model, i.e. functions f_i defined by \mathfrak{T} are of the form

$$X_i = \sum_{j \in \text{Pa}_i} \theta_{ij}^* X_j + N_i, \quad (10)$$

with $\theta_{ij}^* \sim F^*$, with F^* some probability measure with $\text{supp}(F^*) = [-\epsilon, \epsilon], 0 \leq \epsilon \leq 1$, and $N_i \stackrel{i.i.d.}{\sim} \mathcal{N}(\mu, \sigma^2)$. Further assume $\hat{\mathcal{G}} = \mathcal{G}^*$ and $\mathfrak{G} = \mathfrak{F}(\hat{\theta}, \hat{\mathcal{G}})$ also being a linear-additive noise model, where $\hat{\theta}_{ij} \sim \hat{F}$, with \hat{F} another probability measure with $\text{supp}(\hat{F}) = [-1, -\epsilon] \cup [\epsilon, 1]$. We would then find $V_{\text{MD}}^{\mathcal{G}^*, P^{\mathfrak{T}}} \geq V_{\text{MD}}^{\hat{\mathcal{G}}, P^{\mathfrak{G}}}$.

Proof. Denote with $\hat{\mathbf{X}}, \mathbf{X}^*$ the multivariate normal variables introduced by the FCMs $\mathfrak{G}, \mathfrak{T}$, respectively. Since for all CI tests $X \perp\!\!\!\perp Y | Z$ necessary to compute for V_{MD} we have $Z = \emptyset$, c.f. (1), we have $X \perp\!\!\!\perp Y \Rightarrow \rho(X, Y) = 0$. Let us first look at the bivariate case $X \rightarrow Y$. Using (10) and

$N_i \stackrel{i.i.d.}{\sim} \mathcal{N}(\mu, \sigma^2)$ we have $X^* = N_X$ and $Y^* = \theta^* X^* + N_Y$. Thus

$$\begin{aligned} \text{cov}(X^*, Y^*) &= \text{cov}(X^*, \theta^* X^* + N_Y) = \theta^* \text{cov}(X, X) + \text{cov}(X^*, N_Y) \\ &= \theta^* \sigma^2 \end{aligned} \quad (11)$$

$$\rho_{X^*, Y^*} = \frac{\text{cov}(X^*, Y^*)}{\sqrt{\text{Var}(X^*)\text{Var}(Y^*)}} = \frac{\theta^*}{\sqrt{\theta^{*2} + 1}} \quad (12)$$

We can find $\rho_{\hat{X}, \hat{Y}}$ analogously and since $|\theta^*| < |\hat{\theta}|$ it follows $|\rho_{X^*, Y^*}| < |\rho_{\hat{X}, \hat{Y}}|$. Whether or not the smaller correlation leads to a violation of faithfulness depends on the parameter ϵ and the prespecified significance level. The above observation generalizes to arbitrary paths between nodes $i, j \in \text{Anc}_i^{\mathcal{G}}$ since by construction all $|\theta_{kl}^*| < |\hat{\theta}_{kl}|$. \square

F Proofs

F.1 Type I Error Control of the Node Permutation Test

In this section we proof Prop. 4.2 and show that p_{LMC} is a p-value.

Proof. Under the null hypothesis $\hat{\mathcal{G}}$ is a randomly sampled graph from all node permutations. We need to show that then for any type I error control α we have that $\Pr(p_{\text{LMC}}^{\hat{\mathcal{G}}, \mathcal{D}} \leq \alpha) \leq \alpha$. For ease of representation consider an increasing sorting of all permutations by their number of violations yielding $\sigma_1, \dots, \sigma_{|S|}$. For σ_i at least $i/|S|$ permutations have at most as many violations as σ_i , hence $\Pr_{\sigma}(|V_{\text{LMC}}^{\sigma(\hat{\mathcal{G}}), \mathcal{D}}| \leq |V_{\text{LMC}}^{\sigma_i(\hat{\mathcal{G}}), \mathcal{D}}|) \leq i/|S|$. We can view $\hat{\mathcal{G}}$ as being sampled uniformly at random from σ_i . Thus,

$$\Pr(p_{\text{LMC}}^{\hat{\mathcal{G}}, \mathcal{D}} \leq \alpha) = \left| \left\{ \Pr_{\sigma}(|V_{\text{LMC}}^{\sigma(\hat{\mathcal{G}}), \mathcal{D}}| \leq |V_{\text{LMC}}^{\sigma_i(\hat{\mathcal{G}}), \mathcal{D}}|) \leq \alpha \text{ for } 1 \leq i \leq |S| \right\} \right| / |S| \quad (13)$$

$$\leq |\{i/|S| \leq \alpha \text{ for } 1 \leq i \leq |S|\}| / |S| \quad (14)$$

$$= \alpha. \quad (15)$$

\square

F.2 Markov Equivalence Class of Permuted DAGs

In this section we proof Prop. 4.3.

Proof. If $V_{\text{TPa}}^{\mathcal{G}', \mathcal{G}} = \emptyset$, then all parental triples in \mathcal{G}' are d-separated in \mathcal{G} . Further, *all* d-separations in \mathcal{G}' also hold in \mathcal{G} because every valid d-separation statement can be derived from the local $(X_i \perp\!\!\!\perp_{\mathcal{G}} \text{ND}_i^{\mathcal{G}} | \text{Pa}_i^{\mathcal{G}})$ independencies (for a proof using semi-graphoid axioms see e.g. Lauritzen et al. [46], Lauritzen [47]), and the CIs implied by the parental triples imply the local independencies, i.e. for some node i

$$X_i \perp\!\!\!\perp_{\mathcal{G}} X_j | \text{Pa}_i^{\mathcal{G}}, \forall X_j \in \text{Pa}_i^{\mathcal{G}} \Rightarrow X_i \perp\!\!\!\perp_{\mathcal{G}} \text{ND}_i^{\mathcal{G}} | \text{Pa}_i^{\mathcal{G}} \quad (16)$$

\square

G Extending the Node-Permutation Baseline to Violations of Faithfulness

In this section we discuss the difficulty in applying the node-permutation framework to violations of faithfulness instead of violations of local Markov conditions. The difficulty arises from the fact that there is not a well defined way of defining the fraction of violations of faithfulness. The denominator of this fraction should contain all the triplets in the graph that do not entail a d-separation. This is necessary so that any violation of these *non-d-separations* would yield a violation of faithfulness. Nevertheless, the definition of this set of *non-d-separations* is ill-defined for two reasons: First, it does not follow the property of the entailed LMC d-separations that retains the total number of

entailed LMCs invariant to the node-permutations. Second, the size of the conditioning set of these *non-d-separations* is not fixed, and, as such, any decision about it indirectly affects the power of the conditional independence test. The former renders impossible the simplification of the permutation test to use the absolute number of violations in place of the fraction, as the denominator of that fraction will change on every permutation. While this could relatively easily be handled, the latter issue creates the following problem. If we were to pre-define in advance the size of the conditioning set that we would include, then we would impose a prior bias. Even if this was not a problem, the larger conditioning sets would tend to reduce the power of the test, compared to smaller sets for the following reason. Conditioning sets that contain parents of the potential cause node can reduce the variance of the cause if they are strongly correlated with it, and thus reduce the signal to noise ratio [48]. This is something that has higher chances of happening the bigger the conditioning set. To resolve this problem, someone could think of the following two approaches: Either consider only marginal dependencies (with an empty conditioning set for the non-d-separation triplets), or consider performing the permutation test exhaustively for each possible conditioning set size and then combine the resulted p-values. Marginal dependencies are not an appropriate criterion when the given graph entails no marginal d-separations, as the given DAG then is as good as all its permutations. Moreover, the fact that in real datasets we rarely find graphs with marginal independencies makes this issue very relevant. Finally, performing the permutation test separately for each conditioning set size results in a non trivial way of combining the resulting p-values, as each one of them refers to potentially different power of the test as explained above. For the aforementioned reasons, in the current work we focused on introducing a framework that focuses on the fraction of violations of LMCs, exploiting as such, the nice properties that the latter entail.

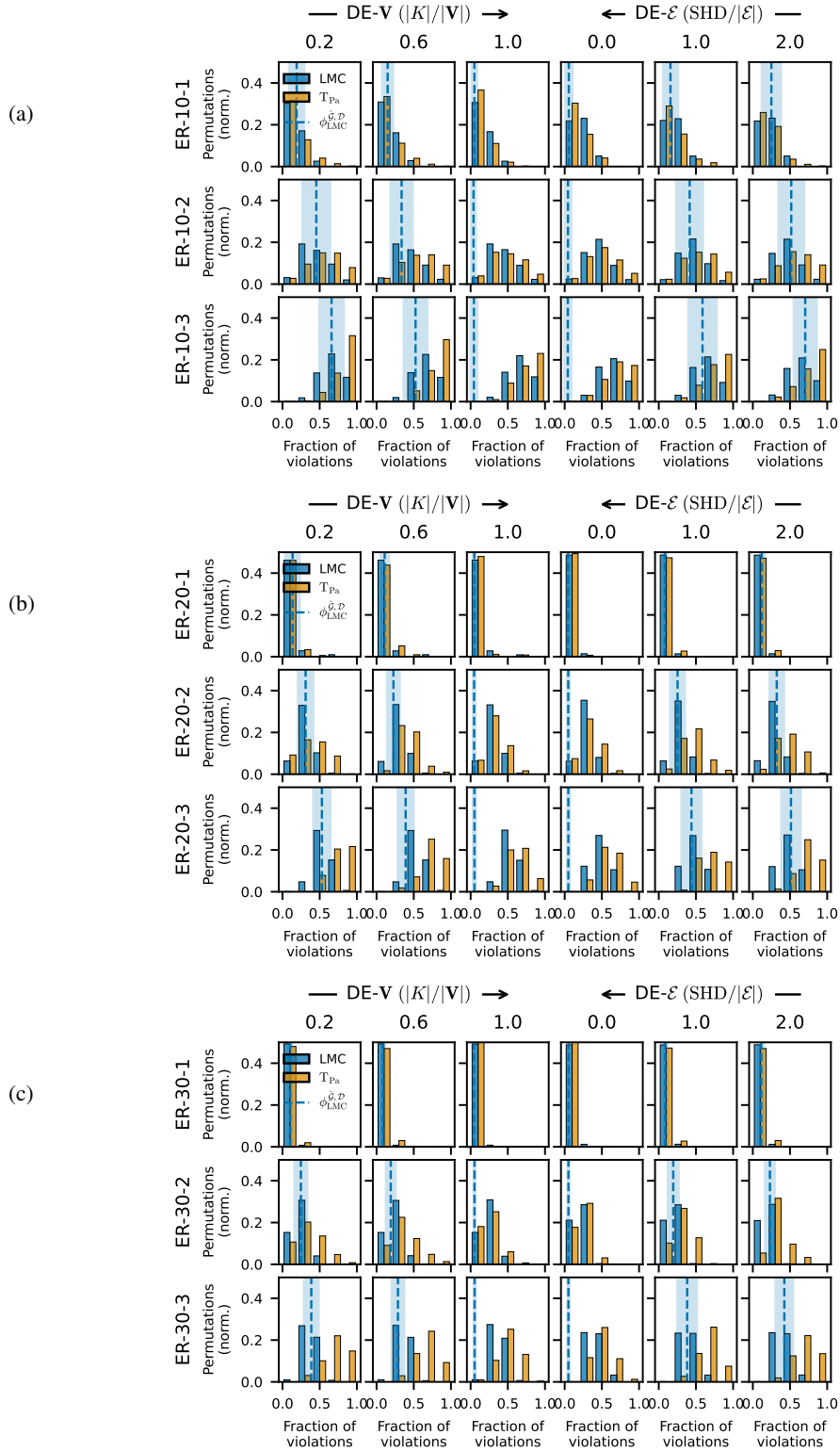


Figure A4: Best viewed in color. Aggregated histograms of LMC (blue) and d-Separation (orange) violations for random ER DAGs with linear-gaussian mechanisms with $n = 10$ (a), $n = 20$ (b), and $n = 30$ (c). The arrows indicate the direction of increasing domain knowledge for the two different domain experts. Additionally, we provide the mean $\phi_{\text{LMC}}^{\mathcal{D}}$ over 50 sampled DAGs (dashed) and standard deviation (shaded).

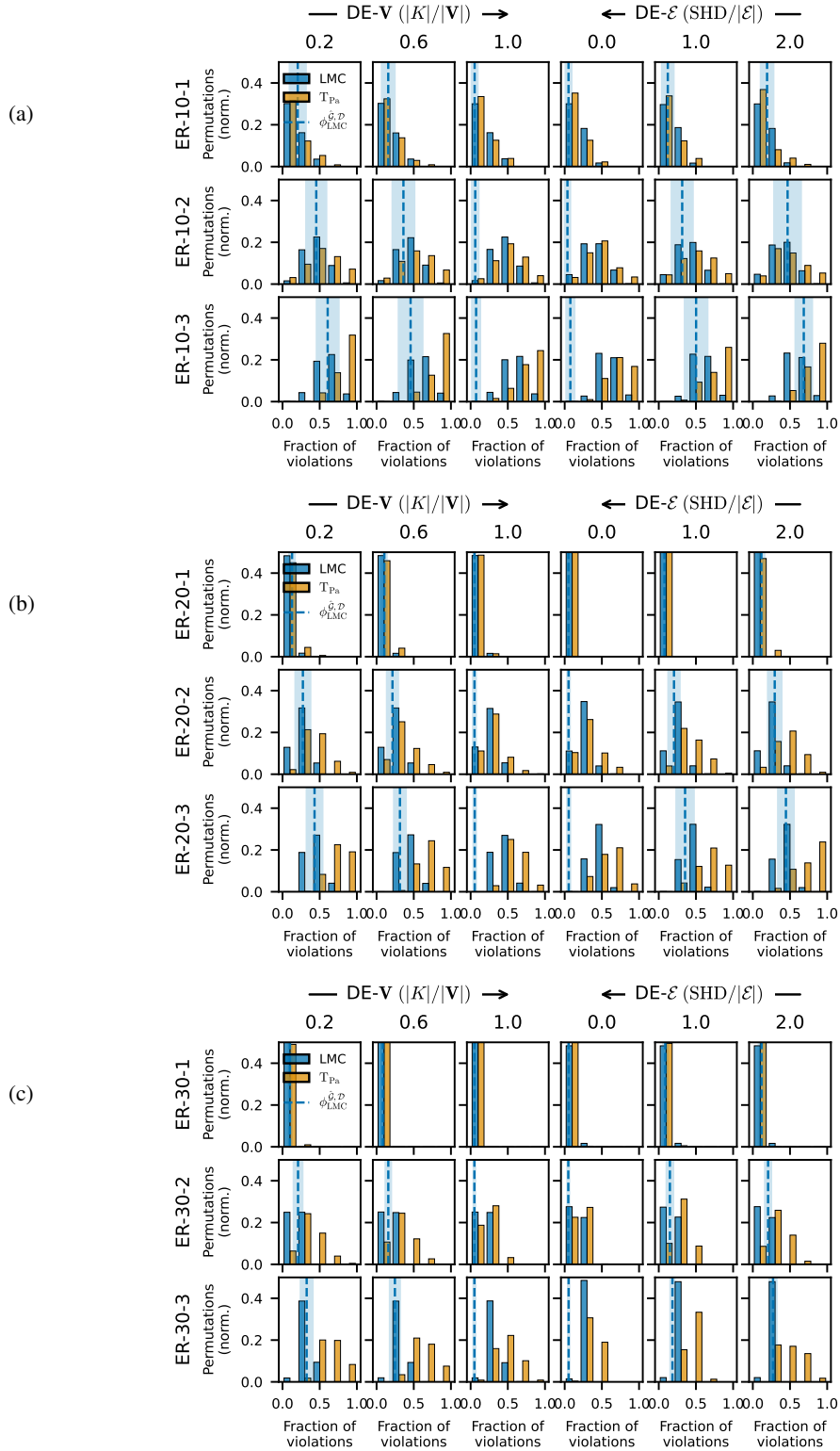


Figure A5: Best viewed in color. Aggregated histograms of LMC (blue) and d-Separation (orange) violations for random ER DAGs with nonlinear mechanisms with $n = 10$ (a), $n = 20$ (b), and $n = 30$ (c). The arrows indicate the direction of increasing domain knowledge for the two different domain experts. Additionally, we provide the mean $\phi_{\text{LMC}}^{\mathcal{G}, \mathcal{D}}$ over 50 sampled DAGs (dashed) and standard deviation (shaded).

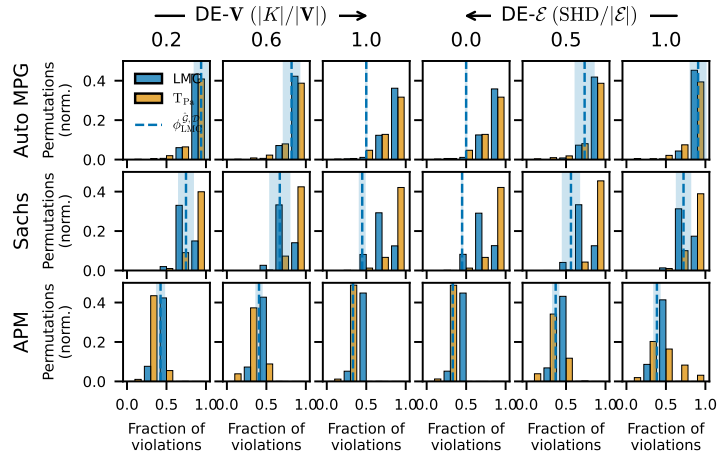


Figure A6: Best viewed in color. Aggregated histograms of LMC (blue) and d-Separation (orange) violations for the Auto MPG [41], Sachs [1], and APM data. The arrows indicate the direction of increasing domain knowledge for the two different domain experts. Additionally, we provide the mean $\hat{\phi}_{\text{LMC}}^{\hat{\mathcal{G}}, \mathcal{D}}$ over 50 sampled DAGs (dashed) and standard deviation (shaded).

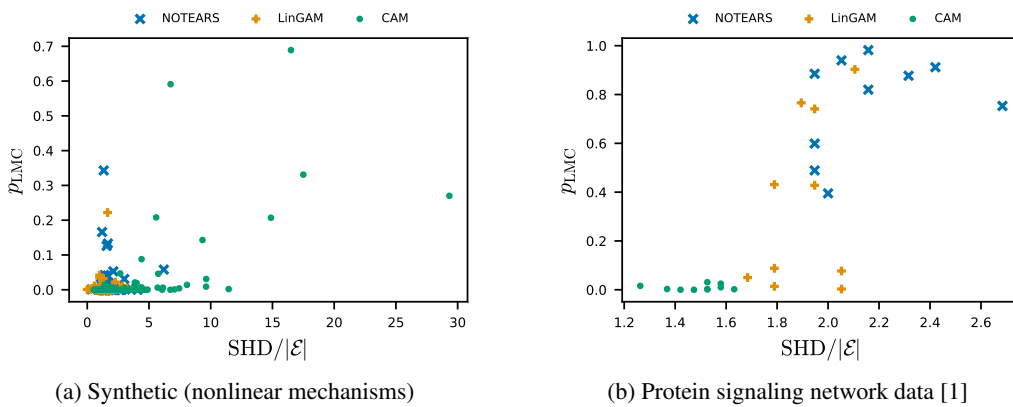


Figure A7: p_{LMC} for $\hat{\mathcal{G}}$ inferred via different causal discovery algorithms on (a) synthetic data and (b) the protein signaling network data.